Available online at www.sciencedirect.com
ScienceDirect
Journal of Power Sources 161 (2006) 133–137
JOURNAL OF POWER SOURCES
www.elsevier.com/locate/jpowsour

Short communication

Electrocatalytic oxidation of methanol by platinum nanoparticles on nickel–chromium alloys

Zhen-Hui Wang *, Ling-Ling Zhang, Kun-Yan Qiu

College of Chemistry and Environmental Science, Henan Key Laboratory for Environmental Pollution Control, Henan Normal University, Xinxiang 453007, PR China

Received 3 February 2006; received in revised form 31 March 2006; accepted 3 April 2006
Available online 5 June 2006

Abstract

In this paper, a novel platinum nanoparticle electrode was prepared by electrodeposition from a platinum salt solution onto a nickel–chromium substrate. The electrocatalytic activity of the electrode for methanol oxidation was studied in acidic solution. Scanning electron microscope (SEM) and cyclic voltammetry were used to characterize the electrode surface and its electrochemical behavior. The results indicated that the platinum nanoparticle modified electrode improved the properties of the substrate material and enhanced the catalytic activity for methanol electrooxidation. The content of platinum metal on the electrode and the cost of the prepared catalyst were remarkably reduced.

Keywords: Platinum microparticle electrode; Nickel–chromium substrate; Electrocatalysis; Methanol oxidation

1. Introduction

Research on the electrocatalytic properties of electrode materials has generally focused on the catalytic oxidation of small organic molecules mainly with the purpose of developing direct small organic molecule fuel cells. Methanol is the one being most intensively investigated among the different small organic molecules [1]. Compared with other cells, the direct methanol fuel cell (DMFC) has the properties of high efficiency and lower polluting emissions. The most active catalyst toward methanol oxidation is platinum or platinum-based alloys in acidic solutions. Numerous modifications of platinum electrodes have been carried out in order to enhance the electrocatalytic oxidation process. Although electrocatalysts based on Pt and Pt–Ru alloys have been developed good activities, the costs of these materials are often very expensive. A great deal of interest has recently been devoted to the development of fuel cell electrocatalysts with the aims of increasing their activity and reducing their cost.

Various multi-component platinum-based catalysts, such as Pt/Rh/Pt [2], polycrystalline and single crystal gold [3], Pd/TiO_2 nanotube [4], PtRu/C [5,6], PtRuRhNi multi-metallic nanoparticle [7], modified nickel hydroxide/glassy carbon electrode [8], Sn-Mo-O [9], Pt-Ru catalysts supported by highly oriented pyrolytic graphite [10], PtRu/C [11], carbon supported Pt–Co alloys [12], Pt-Ru-W [13], Pt-TiO_x/Ti [14], Ni-Ru/C [15], platinized Ti mesh [16], and the electrochemical deposition of Pt-Ru nanoparticles on carbon nanotube electrode [17], have all been used for methanol oxidation.

The purpose of the present work is to study the electrocatalytic oxidation of methanol on a nickel–chromium electrode modified with platinum nanoparticles by an electrochemical method, in order to obtain a less expensive and more active electrocatalyst. The platinum nanoparticle electrode showed excellent catalytic activity towards methanol oxidation compared with a pure platinum electrode. Under the same conditions, the catalytic activity of the former is 30 times higher than that of the later. Moreover, the dosage of platinum metal in the catalyst is remarkably reduced, the cost of prepared catalyst is therefore greatly decreased, and the procedure is very simple.

2. Experimental

2.1. Instruments and reagents

Electrochemical measurements were carried out with a CHI electrochemical workstation (Shanghai, China). A three-

* Corresponding author. Tel.: +86 373 3326335; fax: +86 373 3326336.
E-mail address: wang728@public.xxptt.ha.cn (Z.-H. Wang).

0378-7753/$ – see front matter © 2006 Elsevier B.V. All rights reserved.
doi:10.1016/j.jpowsour.2006.04.022

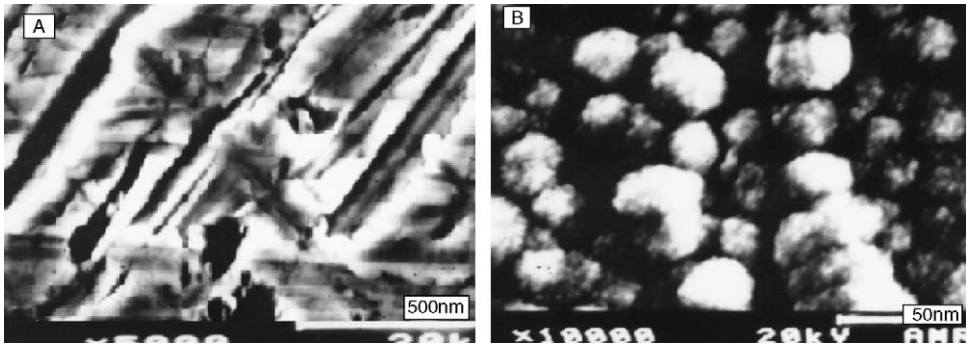

Fig. 1. Scanning electron micrographs of nickel–chromium substrate (A) and the platinum nanoparticles (B).

electrode system comprised of platinum nanoparticle working electrode, platinum sheet counter-electrode, and a saturated calomel electrode (SCE) as the reference electrode. A pure platinum electrode with 2.5 mm diameter (0.049 cm^2) was used as comparative test. The scanning electron microscope (SEM) image of the platinum nanoparticle film was obtained with an AMRAY-1000B scanning electron microscope (AMRAY Co., USA).

Potassium chloroplatinate and methanol (Beijing, China) were used. All the chemicals were analytical reagent grade, and all solutions were prepared with doubly distilled water and stored in the dark. All the experiments were carried out at room temperature.

2.2. Electrode preparation

A nickel–chromium alloy rod with a 2.48 mm diameter (0.048 cm^2) and a 100 mm length was sealed in a matched glass tube. One end was used as the electrode connection held out of the glass tube, the other one as the working surface. The surface was polished with 0.05 μm alumina slurry and then cleaned ultrasonically in HNO_3 (1:1) absolute ethanol, doubly distilled water successively and then allowed to dry at room temperature. After that, the electrochemical pretreatment was carried out in 0.007 M K_2PtCl_6 + 0.5 M H_2SO_4 solutions by 50 times (about 2 h) successively cyclic scan from −0.2 to 0.5 V with a scan rate of 10 mV s^{-1}. Platinum was uniformly electrodeposited onto the surface of the nickel–chromium alloy substrate. Then, the electrode was rinsed with distilled water before use.

3. Results and discussion

3.1. Distribution of platinum nanoparticles on the substrate surface

The properties of electrode materials intensively affect the electrochemical reaction. The nickel–chromium alloy is a very hard metal. It is corrosion-resistant, has few crystal irregularities, has a high mechanical strength, wide electrochemical potential windows and good stability. Because of its higher resistivity, the nickel–chromium alloy shows inertia to many electrochemical reactants when used as a working electrode. The alloy materials cannot serve as the working electrode directly for methanol oxidation. However, experiments proved that the electrochemical properties of the nickel–chromium substrate can be changed by electrodeposition of highly dispersed platinum nanoparticles on its surface. Fig. 1A shows the SEM image of the nickel–chromium substrate. It can be seen that there are some regular grooves on the substrate. Its surface is mainly composed of a nickel–chromium solid solution, and $NiCr_2O$ spinels by X-ray diffraction (XRD) spectral analysis. Fig. 1B shows the SEM image of the platinum deposited on nickel–chromium substrate. The round-shaped, white spots are the platinum nanoparticles. Obviously, the distribution of the platinum nanoparticles on the nickel–chromium surface is uniform. Repeating the electrodeposition process under the same conditions, the results are the same, indicating that the platinum nanoparticles deposited on the nickel–chromium substrate had a good reproducibility.

3.2. The electrochemical characteristic of platinum nanoparticle electrode

The electrochemical properties of the platinum nanoparticle electrode were examined by cyclic voltammetry in 2.0 mM $K_4[Fe(CN)_6]$ + 1.0 M KNO_3 solutions. Fig. 2 shows the cyclic voltammograms of $K_4[Fe(CN)_6]$ measured with different electrodes. At the nickel–chromium electrode, only the oxidation peak of $K_4[Fe(CN)_6]$ appears at about 0.5 V without a corresponding reduction peak (curve a), indicating that

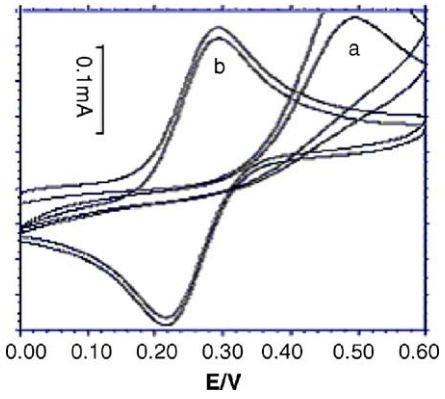

Fig. 2. Repetitive cyclic voltammograms of $K_4[Fe(CN)_6]$ on the base electrode before and after electrodeposited platinum: (a) before electrodeposition and (b) after electrodeposition. Scan rate, 200 mV s^{-1}; $K_4[Fe(CN)_6]$, 2 × 10^{-3} M; supporting electrolyte, 1.0 M KNO_3.

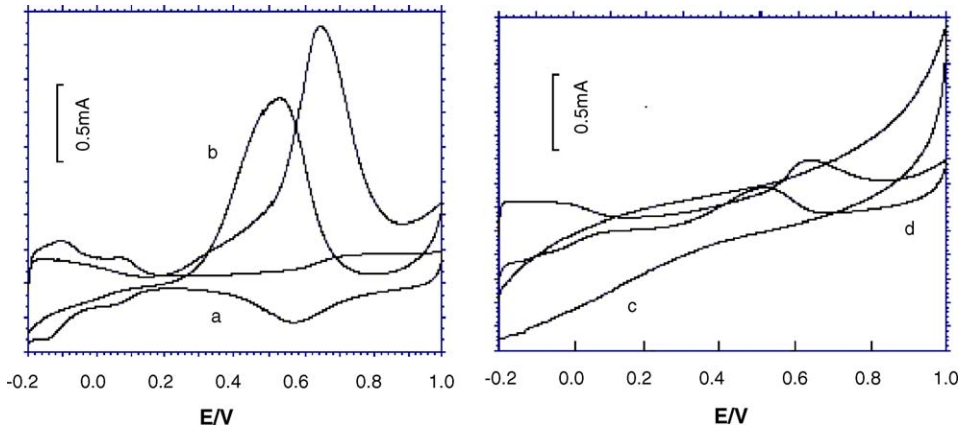

Fig. 3. The cyclic voltammograms of methanol oxidation on different electrodes. (a) Pt nanoparitcle electrode at 0.5 M $HClO_4$; (b) (a) + 0.1 M methanol; (c) bare nickel–chromium electrode + 0.1 M methanol; (d) pure platinum electrode at 0.1 M methanol. C_{CH_3OH}, 0.1 M; υ, 100 mV s^{-1}; base electrolyte, 0.5 M $HClO_4$.

the oxidation of $K_4[Fe(CN)_6]$ at the nickel–chromium electrode exhibits irreversible electrode process. A pair of well-defined oxidation–reduction peaks were observed at the platinum nanoparticle electrode (curve b) under the same conditions. The oxidation peak potential appears at 0.28 V and the reduction peak at 0.22 V, respectively. The potential difference of both peaks approaches 60 mV, and the ratio of the oxidation to reduction peak currents equals 1, which is a characteristic of a totally reversible electrode process [18]. Compared with the bare nickel–chromium electrode, the oxidation peak potential of the Pt nanoparticle electrode negatively shifted to 220 mV. These results reveal that the electrochemical properties of the platinum nanoparticle electrode are quite similar to pure platinum electrode. Indicating that the platinum nanoparticles deposited on the nickel–chromium substrate can be used as working electrode. According to the Randles–Ševčik equation [18], calculating the true surface area of the platinized platinum electrode equals 0.066 cm^2 by five times successively cyclic potential scans, while the geometric area is 0.048 cm^2. The result is the same as calculated from the charge for a monolayer formation of adsorbed hydrogen in 1.0 M H_2SO_4 solution using 210 $\mu C\ cm^{-2}$ as the conversion factor.

3.3. The electrocatalysis oxidation of methanol

The electrocatalytic activity of the Pt nanoparticle electrode on methanol oxidation was investigated by cyclic voltammetry. Typical cyclic voltammograms are shown in Fig. 3. Curve a represents the voltammogram of Pt nanoparticle electrode in 0.5 M $HClO_4$ solution without methanol. It can be seen that there are two pairs of oxidation–reduction peaks at about −0.1 V, which are attributed to the adsorption/desorption of hydrogen in acid solution. The formation of platinum oxide appears at 0.7 V and its reduction peak potential at 0.56 V, respectively. The figure is similar to that represented by Breiter [19] and Feltham and Spioro [20]. The oxidation–reduction peaks of methanol are observed at 0.64 and 0.52 V (curve b in Fig. 3). Compared with curve a, the adsorption/desorption peaks of hydrogen at −0.1 V are decreased, obviously. This is mainly because the competitive absorption of methanol at Pt nanoparticle surface decreases the adsorption quantity of hydrogen. The oxidation peak at 0.64 V is attributed to the oxidative removal of adsorbed/dehydrogenated methanol fragments by oxygen-containing species PtOH. During this process, CO, CO_2, HCOOH, HCOH and $HCOOCH_3$ are formed and CO molecules readsorb, poisoning the electrode surface [1]. The peak current at 0.52 V is attributed to the re-oxidation of CO and other adsorbed species.

The curve c in Fig. 3 is the voltammogram of nickel–chromium electrode in 0.5 mol L^{-1} $HClO_4$ containing 0.1 M of methanol. No current signal of methanol oxidation is observed, indicating that the nickel–chromium electrode is inert for methanol electrooxidation. Curve d in Fig. 3 shows the voltammogram of pure Pt electrode under the same conditions. From curve d, it can be seen that the adsorption/desorption peaks of hydrogen appear at −0.1 V, the oxidation–reduction peaks of methanol oxidation at 0.64 and 0.52 V, respectively. But, the current density of pure Pt electrode for methanol oxidation is lower than that of the Pt nanoparticle electrode. All of these indicate that Pt nanoparticles possesses many active locations and excellent catalytic capability to methanol electrooxidation.

The peak current, i_p is proportional to the square root of scan rate ν (Fig. 4) indicating that the electrochemical oxidation reaction of methanol is a diffusion-controlled process.

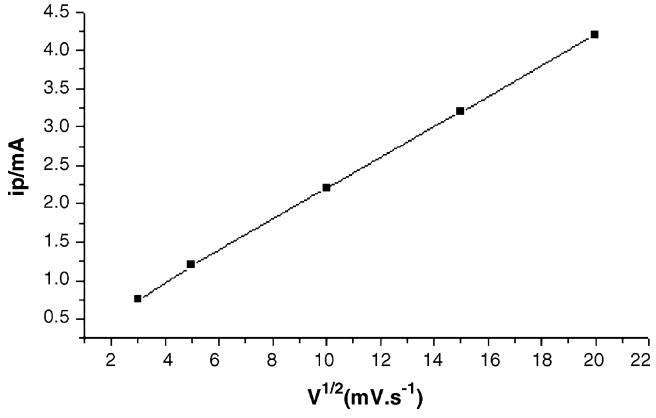

Fig. 4. Relationship of the current density of methanol oxidation with the square of the scan rate. Other conditions as in Fig. 3.

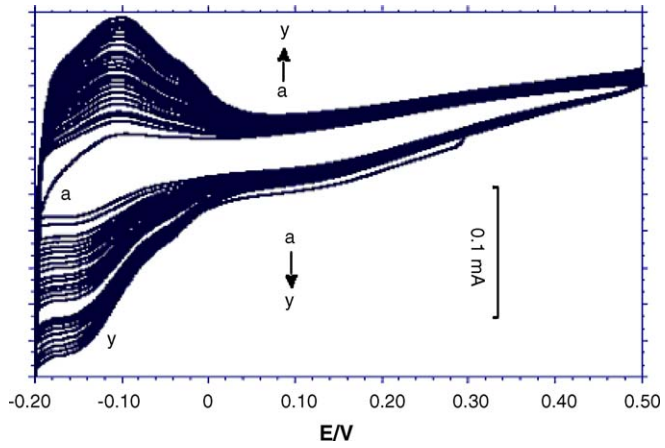

Fig. 5. Cyclic voltammograms of electrodeposited platinum on a nickel–chromium substrate in 0.007 M K_2PtCl_6 + 0.5 M H_2SO_4 solution; scanning rate, 10 mV s^{-1}. a → y cyclic scanning degrees increase in turn.

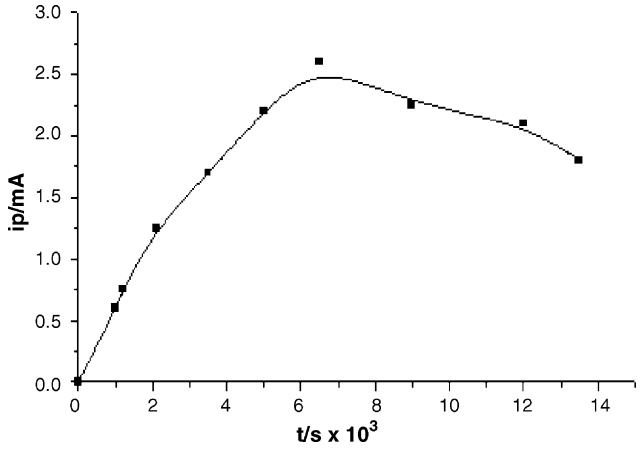

Fig. 6. The relationship between peak currents of methanol oxidation and the cyclic scan time of depositing platinum. Other conditions as in Fig. 3.

3.4. Size effects of Pt nanoparticles on methanol electrocatalyzing

The size of the Pt nanoparticles deposited on the nickel–chromium substrate affected the current density of methanol oxidation. Generally, small particle size and high dispersion of the catalyst may result in a large active catalyst surface area for methanol oxidation. The mean size of the Pt nanoparticles increased with increasing the amount of platinized platinum [21]. This implied that the size of Pt nanoparticles depended on the potential, cyclic time or cycle number, and the deposition potential range. Experiments proved that the optimization deposition potential range was −0.20 and 0.50 V. The amount of Pt nanoparticle deposited was increased with increasing of the cyclic scan time. Fig. 5 shows the successive cyclic voltammograms of electrodeposited platinum at the surface of nickel–chromium from −0.2 to 0.5 V. No distinct adsorption/desorption peaks of hydrogen can be observed at the beginning. This is because Pt nanoparticles deposited at the nickel–chromium surface are very few at first. Then, two pairs of oxidation–reduction peaks, which are the adsorption/desorption peaks of hydrogen, appeared at −0.1 V. The peak currents were increased with increasing cycle number, and their peak potentials do not change with successive cyclic scans. This indicates that Pt nanoparticles can be steadily formed on the nickel–chromium substrate in a given potential scan period.

For obtaining platinum deposits, a procedure described in references [22,23] was used. The platinum electrodeposits was characterized by calculating the following parameters such as the true surface (S_{trus}, cm^2), the specific surface ($S_{sp} = S_{true}/m_{pt}$, $m^2\ g^{-1}$), the roughness factor ($\gamma = S_{true}/S_{geom}$), the platinum loadings (m_{pt}, μg) and the average diameter of platinum particles ($d = 6m_{pt}/\rho S_{true}$ (nm), where ρ is platinum specific density, 21.4 g cm^{-3}). The platinum loadings were determined from the charge during the sweep provided that the coulombic efficiency was 100%. The true surface area of the Pt nanoparticle electrode was calculated from the reduction charge of absorbing hydrogen and the oxidation charge of ferrocyanide. These parameters are summarized in Table 1.

It can be seen from Table 1 that the platinum electrodeposit has the largest true surface and the appropriate size, and the best electrochemical response for methanol electrooxidation was also observed at Pt nanoparticle electrode with the electrodeposit of 30 cyclic potential scans.

The cyclic time of platinized Pt nanoparticles and the electrocatalytical properties on methanol oxidation were examined (Fig. 6). As shown in Fig. 6, the current density of methanol oxidation increased with increasing cycle time, indicating that the coverage of Pt nanoparticles on the nickel–chromium surface increased with increasing cyclic scan time, which led to an increase of the peak currents for methanol oxidation. According to theory [24], it is considered that the metal platinum electrodeposition is a crystal growth process. The configuration and surface structure of platinum crystals are controlled by the experimental conditions, especially the potential range of deposition. It can be seen from Fig. 6 that the current density rapidly increases and then decays to a limiting value within 14,000 s. When the time for depositing platinum particles approaches

Table 1
Parameters of platinum electrodeposit on the polished Pt electrode

Number of potential cycles	Platinum loading (μg cm^{-2})	Roughness factor (γ)	True surface (cm^2)	Specific surface ($m^2\ g^{-1}$)	Particles diameter (nm)
5	0.54	1.4	0.066	11.22	22.9
20	1.28	4.7	0.226	17.66	15.9
30	4.88	7.3	0.350	7.17	39.1
50	9.92	6.8	0.324	3.27	85.8

5000–7000 s (about 30–50 cyclic potential scans), the oxidation current density of methanol is the highest. This implies that the coverage of platinum crystal on the substrate surface reaches a maximum value, and the reaction rate of methanol electrooxidation also rapidly reaches a maximum value. As the cyclic scan time exceeds 7500 s, or exceeds 50 cyclic potential scans, the peak current of methanol oxidation was rapidly decreased, indicating that the catalytic activity of the electrode and reaction rate decreased. This is because the size of deposited platinum grows into a bulk material and loses the property of a Pt nanoparticle electrode interface. Therefore, in order to get uniform Pt nanoparticle crystals, the electrodeposition potential range and cyclic time, or times, should be carefully controlled.

4. Conclusion

Highly dispersed Pt nanoparticles were electrodeposited onto a nickel–chromium substrate by cyclic voltammetry from −0.2 to 0.5 V in 0.5 M H_2SO_4 solutions with potassium chloroplatinate. The electrochemical properties of the Pt nanoparticle electrode were examined in 2 mM $K_4[Fe(CN)_6]$ + 1.0 M KNO_3 aqueous solution and the electrocatalytical properties for methanol electrooxidation were investigated by voltammetry in a 0.5 M $HClO_4$ solution. The corresponding results showed that the Pt nanoparticle electrode exhibited a better electrocatalytic activity than a pure Pt electrode. The catalytic activity is 30 times higher than that of a pure platinum electrode under the same experimental conditions. Moreover, the cost of preparing a Pt nanoparticle catalyst was greatly reduced.

Acknowledgements

This work was supported by the Nature Science Foundation of Henan province, People's Republic of China (Grant No. 0311021000), Key Laboratory of Environmental Science and Engineering, Education Commission of Henan Province.

References

[1] T. Iwasita, Electrochem. Acta 47 (2002) 3663–3674.
[2] R.T.S. Oliveira, M.C. Santos, B.G. Marcussi, P.A.P. Nascente, L.O.S. Bulhoes, E.C. Pereira, J. Electroanal. Chem. 575 (2005) 177–182.
[3] Z. Borkowska, A. Tymosiak-Zielinska, G. Shul, Electrochim. Acta 49 (2004) 1209–1220.
[4] M. Wang, D.-J. Guo, H.-L. Li, J. Solid State Chem. 178 (2005) 1996–2000.
[5] S.Lj. Gojkovic, T.R. Vidakovic, D.R. Durovic, Electrochim. Acta 48 (2003) 3607–3614.
[6] E.V. Spinace, A.O. Neto, M. Linardi, J. Power Sources 129 (2004) 121–126.
[7] K.-W. Park, J.-H. Choi, S.-A. Lee, C. Pak, H. Chang, Y.-E. Sung, J. Catal. 224 (2004) 236–242.
[8] A.A. EI-Shafei, J. Electroanal. Chem. 471 (1999) 89–95.
[9] N. Graciela Valente, L.A. Arrua, L.E. Cadus, Appl. Catal. A-Gen. 205 (2001) 201–214.
[10] C.-H. Lee, C.-W. Lee, D.-I. Kim, S.-E. Bae, Int. J. Hydrogen Energy 27 (2002) 445–450.
[11] G. Wu, L. Li, B.-Q. Xu, Electrochim. Acta 50 (2004) 1–10.
[12] J.R.C. Salgado, E. Antolini, E.R. Gonzalez, Appl. Catal. B-Environ. 57 (2005) 283–290.
[13] M. Umeda, H. Ojima, M. Mohamedi, I. Uchida, J. Power Sources 136 (2004) 10–15.
[14] H. Yang, T. Lu, C. Lu, J. Lu, G. Sun, Chem. J. Chin. Univ. 21 (2000) 1283–1287.
[15] M.A. Abdel Rahim, R.M. Abdel Hameed, M.W. Khalil, J. Power Sources 135 (2004) 42–51.
[16] E.H. Yu, K. Scott, R.W. Reeve, L. Yang, R.G. Allen, Electrochim. Acta 49 (2004) 2443–2452.
[17] Z. He, J. Chen, D. Liu, H. Zhou, Y. Kuang, Diam. Relat. Mater. 13 (2004) 1764–1770.
[18] A.J. Bard, L.R. Faulkner, Electrochemical Methods Fundamentals and Applications, second ed., John Wiley & Sons, Inc., New York, 1980, p. 218.
[19] M.W. Breiter, Electrochim. Acta 6–7 (1963) 447–456.
[20] A.M. Feltham, M. Spioro, Chem. Rev. 94 (1971) 1025–1032.
[21] Y. Takasu, T. Iwazaki, W. Sugimoto, Y. Murakami, Electrochem. Commun. 2 (2000) 671–674.
[22] J.H. Ye, P.S. Fedkiw, Elactrochim. Acta 41 (1996) 221–231.
[23] A.A. Mikhaylova, O.A. Khazova, V.S. Bagotzky, J. Electroanal. Chem. 480 (2000) 225–232.
[24] E. Budevski, G. Staikov, W.J. Lorenz, Electrochim. Acta 45 (2000) 2559–2574.